# Finite Volume Modelling of an Axisymmetric Cylindrical Fin using Python

**Article** · March 2022

DOI: 10.5281/zenodo.6345803



**4 authors:**

Pankaj Dumka
Jaypee University of Engineering and Technology
**52** PUBLICATIONS **586** CITATIONS
SEE PROFILE

Saksham Sharma
Jaypee University of Engineering and Technology
**7** PUBLICATIONS **19** CITATIONS
SEE PROFILE

Harshit Gautam
Jaypee University of Engineering and Technology
**7** PUBLICATIONS **19** CITATIONS
SEE PROFILE

Dr. Dhananjay R. Mishra
Jaypee University of Engineering and Technology
**104** PUBLICATIONS **909** CITATIONS
SEE PROFILE

HBRP PUBLICATION

Research and Applications of Thermal Engineering
Volume 4 Issue 3
DOI: https://doi.org/10.5281/zenodo.6345803

# Finite Volume Modelling of an Axisymmetric Cylindrical Fin using Python

***Pankaj Dumka*, Saksham Sharma, Harshit Gautam, Dhananjay R. Mishra***
*Department of Mechanical Engineering, Jaypee University of Engineering and Technology, Guna, Madhya Pradesh.*

****Corresponding Author***
***E-mail Id:-****p.dumka.ipec@gmail.com*

***ABSTRACT***

*In this research article an attempt has been made to numerically examine the performance of an axisymmetric fin. The finite volume approach has been adopted to discretize the governing equations on a uniformly spaced grid. Successive over relaxation has been used to solver the nodal equations iteratively to arrive at converged solution for temperature variation within the domain. Influence of varying thermal conductivity of fin material and surrounding convective heat transfer has been examined and reported. A python code has been written in Jupyter notebook for solving the finite volume problem.*

***Keywords:-*** *CFD, Fin, Finite Volume, Python, Partial differential equations, Heat transfer*

**NOMENCLATURE**

| | |
|---|---|
| R | Radius of fin (m) |
| r | radial location (m) |
| z | Longitudinal direction of fin (m) |
| T | Temperature (°C) |
| $T_o$ | Base temperature of fin (°C) |
| $\theta = T - T_\infty$ | Temperature difference (°C) |
| $T_\infty$ | Ambient temperature (°C) |
| $V$ | Volume ($m^3$) |
| $A$ | Area ($m^2$) |
| **k** | Thermal conductivity (W/m-K) |
| h | Convective heat transfer coefficient ($W/m^2$-K) |
| **Subscripts** | |
| e | East face |
| w | West face |
| n | North face |
| s | South face |
| E | Eastern cell centre |
| W | Western cell centre |
| N | Northers cell centre |
| S | Southern cell centre |
| **Greek** | |
| $\beta$ | Relaxation factor |

  

Research and Applications of Thermal Engineering
Volume 4 Issue 3
DOI: https://doi.org/10.5281/zenodo.6345803

## INTRODUCTION

Fins are extended surfaces moving perpendicular to the primary surface used to transmit heat by modes of conduction and convection primarily. Fins can be categorized into varieties of geometry such as constant area straight fin, variable area straight fin, pin fin, and annular fin.

Fins can be mounted on internal or external sides of the surface depending upon the purpose of the operation. Fins are generally utilized to increase the surface area and thus increase heat transfer rate. For the most part, Fins are used in air-cooled IC engines and radiators for cooling in automobiles. In electronics, it is used in different semiconductor devices electronic components; the use of pin fin is common in computers.

Various researchers have previously contributed to examining different types of fins, their nature, purpose, and thermal performance of multiple fins have been extensively studied. Bahadur & Bar-cohen,[1Freported an analytical solution for cylindrical pin fin with orthotropic thermal conductivity. They numerically validated the heat transfer rate equation based on thermal conductivity, aspect, and Biot numbers.

They reported that the heat transfer rate increases with the radical Biot number. Kumar et al. [2]wrote an analysis of cylindrical pin fin with natural and forced convection heat transfer.

They have reported that the increase in temperature gradient value of Prandtl number decreases in natural convection while values of Grashof number and Nusselt number increase[3].

The efficiency of the pin fin is observed to decrease with an increase in a temperature gradient in natural and forced convection. Maji & Choubey, 2020[4]reported a review of heat transfer enhancement using fins for various thermophysical and geometrical parameters. Hatami et al.[5]reported higher heat generation rates leads to higher fin temperature, which was compared and calculated using the Darcy model. They used different analytical methods such as differential transformation, collocation, and least square to predict the temperature distribution in porous fin.

Lane and Heggs[6] have developed a generalized mathematical model to capture the temperature distribution along tapered, trapezoidal, and inverted trapezoidal fins. Effect of varying ambient temperature conditions and fin geometry on the performance characteristics of fin have been studied by Nnanna et al. [7].

Mohankumar et al. [8] have reported a computational analysis of fin with different geometries viz bar and stepped (with and without indentations) fins. Rao and Somkuwar [9] have investigated the tapered fin heat transfer under the condition of natural convection. The fin taper they have varied from 1 to 3° with heat source power variation from 5 to 70 W.

In this manuscript, an investigationon axisymmetric cylindrical fin using the finite volume approach has been done. The fin has been examined for different materials and varying convective heat transfer coefficients.

## MATHEMATICAL MODELLING AND ALGORITHM

Figure 1. shows the schematic of cylindrical pin fin and its axisymmetric view. In this analysis instead of directly finding the temperature its difference with the atmospheric temperature has been evaluated ($\theta = T - T_\infty$). This will help in writing the equations more compactly.

Research and Applications of Thermal Engineering
Volume 4 Issue 3
DOI: https://doi.org/10.5281/zenodo.6345803

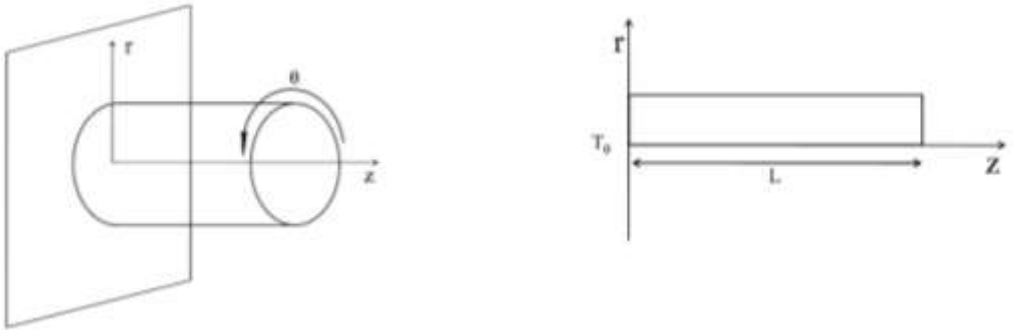


(a) Fin (b) Axisymmetric view

***Fig.1:-****Schematic of fin and its axisymmetric view*

**Finite Volume Discretization**

For the analysis following assumptions are made:

- Steady state
- Axisymmetric condition
- Fixed base temperature $T_0$
- Convection at the fin tip

The steady state 2d heat conduction heat conduction equation can be written as[3]:

$$\frac{1}{r}\frac{\partial}{\partial r}\left(r\frac{\partial\theta}{\partial r}\right)+\frac{\partial^2\theta}{\partial z^2}=0 \quad (1)$$

Multiplying both side by r we get:

$$\frac{\partial}{\partial r}\left(r\frac{\partial\theta}{\partial r}\right)+r\frac{\partial^2\theta}{\partial z^2}=0 \quad (2)$$

As the second derivative is with respect to z, so r is a constant for this expression which can be moved inside the derivative as follows:

$$\frac{\partial}{\partial r}\left(r\frac{\partial\theta}{\partial r}\right)+\frac{\partial^2(r\theta)}{\partial z^2}=0 \quad (3)$$

To solve the above equation finite volume approach has been adopted in this manuscript. A uniform structured grid has been used for the discretization. Figure 2 shows the rectangular grid structure.

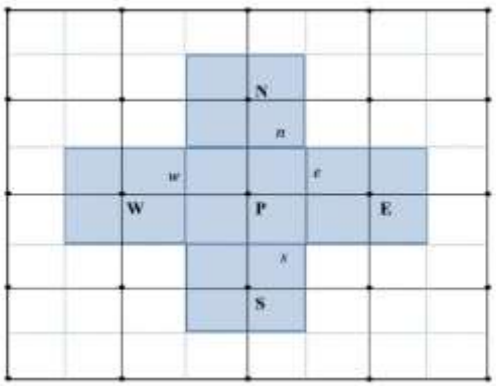


***Fig.2:-****Finite volume rectangular grid*

Research and Applications of Thermal Engineering
Volume 4 Issue 3
DOI: https://doi.org/10.5281/zenodo.6345803

Integrating Eq. 3 considering unit width into the paper we get:

$$\int_V \frac{\partial}{\partial r}\left(r\frac{\partial \theta}{\partial r}\right)dV + \int_V \frac{\partial^2(\theta r)}{\partial z^2}dV = 0 \quad (4)$$

Applying Gauss divergence theorem[10] to convert volume into area integral one can get:

$$\int_A \left(r\frac{\partial \theta}{\partial r}\right)dA + \int_A \frac{\partial(\theta r)}{\partial z}dA = 0 \quad (5)$$

Integrating over P cell we get[10]:

$$\left(A\, r\frac{\partial \theta}{\partial r}\right)_n - \left(A\, r\frac{\partial \theta}{\partial r}\right)_s + \left(A\frac{\partial(\theta r)}{\partial z}\right)_e - \left(A\frac{\partial(\theta r)}{\partial z}\right)_w = 0 \quad (6)$$

It is assumed that in between the nodes the temperature variation is continuous (i.e., piece wise linear[11]) and the slope at the face is obtained by central difference as:

$$A_n r_n\left[\frac{\theta_N-\theta_P}{\Delta r}\right] - A_s r_s\left[\frac{\theta_P-\theta_S}{\Delta r}\right] + A_e\left[\frac{(r\theta)_N-(r\theta)_P}{\Delta z}\right] - A_w\left[\frac{(r\theta)_P-(r\theta)_W}{\Delta z}\right] = 0 \quad (7)$$

$$r_e = r_E = r_P = r_w = r_W \quad (8)$$

$$r_n = \frac{r_N+r_P}{2} \quad (9)$$

$$r_s = \frac{r_P+r_S}{2} \quad (10)$$

$$\frac{A_n r_n}{\Delta r}\theta_N - \frac{A_n r_n}{\Delta r}\theta_P - \frac{A_s r_s}{\Delta r}\theta_P + \frac{A_n r_n}{\Delta r}\theta_S + \frac{A_e r_E}{\Delta z}\theta_E - \frac{A_e r_P}{\Delta z}\theta_P - \frac{A_w r_P}{\Delta z}\theta_P + \frac{A_w r_W}{\Delta z}\theta_W = 0 \quad (11)$$

On rearranging the above equation, we get:

$$\left(\frac{A_n r_n}{\Delta r} + \frac{A_s r_s}{\Delta r} + \frac{A_e r_P}{\Delta z} + \frac{A_w r_P}{\Delta z}\right)\theta_P = \left(\frac{A_n r_n}{\Delta r}\theta_N + \frac{A_s r_s}{\Delta r}\theta_S + \frac{A_e r_E}{\Delta z}\theta_E + \frac{A_w r_W}{\Delta z}\theta_W\right) \quad (12)$$

Using Eq. 8 the Eq. 12 becomes:

$$\left(\frac{A_n r_n}{\Delta r} + \frac{A_s r_s}{\Delta r} + \frac{A_e r_E}{\Delta z} + \frac{A_w r_W}{\Delta z}\right)\theta_P = \left(\frac{A_n r_n}{\Delta r}\theta_N + \frac{A_s r_s}{\Delta r}\theta_S + \frac{A_e r_E}{\Delta z}\theta_E + \frac{A_w r_W}{\Delta z}\theta_W\right) \quad (13)$$

Let $a_E = \frac{A_e r_E}{\Delta z}, a_W = \frac{A_w r_W}{\Delta z}, a_N = \frac{A_n r_n}{\Delta r}, a_S = \frac{A_s r_s}{\Delta r}$ and $a_P = a_E + a_W + a_N + a_S$, then the Eq. 13 becomes:

$$a_P\theta_P = (a_N\theta_N + a_S\theta_S + a_E\theta_E + a_W\theta_W) \quad (14)$$

Now, Eq. 14 is be solved at each node with the boundary conditions as mentioned in Table. 1.

***Table 1:****-Different boundary conditions and their discretized version.*

| **Boundary** | **Boundary condition** | **Discretized boundary condition** |
|---|---|---|
| Left boundary ($z = 0$) | $\theta = \theta_0 = (T_0 - T_\infty)$ Where, $T_0$ is the base temperature and $T_\infty$ is the ambient temperature. | $\theta_{boundary} = \theta_0$ |
| Right boundary ($z = \ell$) | $-\left(k\frac{\partial \theta}{\partial z}\right)_{z=\ell} = h \times \theta$ (Fourth assumptions) | $\theta_{boundary} = \frac{\theta_{inner}}{\left(1+\frac{h\Delta z}{k}\right)}$ |
| Bottom boundary ($r = 0$) | $\frac{\partial \theta}{\partial r} = 0$ (Second assumption) | $\theta_{boundary} = \theta_{inner}$ |
| Top boundary ($r = R$) | $-\left(k\frac{\partial \theta}{\partial r}\right)_{r=R} = h \times \theta$ | $\theta_{boundary} = \frac{\theta_{inner}}{\left(1+\frac{h\Delta r}{k}\right)}$ |

Research and Applications of Thermal Engineering
Volume 4 Issue 3
DOI: https://doi.org/10.5281/zenodo.6345803

**Algorithm and Solution Procedure**

In this manuscript iterative method i.e.,successive over relaxation (SOR) has been adopted[12]. In SOR temperature field ($\theta$) is guessed and then Eq. 14 is solved to obtain an improved field of $\theta$. Successive iteration of the above step will lead to a solution that is close to the result.In this algorithm only one set of dependent variables i.e., ($\theta$) is held in the computer memory. At the start these represent the value of dependent variable from previous iteration or guess value. With each gird point visited by the program the corresponding value of $\theta$ is changed as follows:

$$\theta_P = \theta_P + \left(\frac{\beta}{a_P}\right) \times (a_N\theta_N + a_S\theta_S + a_E\theta_E + a_W\theta_W - a_P\theta_P) \quad (15)$$

Where, $\beta$ is the relaxation factor. For $\beta < 1$ the scheme is called as under relaxation, if $\beta > 1$ then it is called over relaxation, and when $\beta = 1$ the SOR is called as Gauss-Seidel. For non-linear behaviour (as in N-S equation) under relaxation is used whereas, for linear problems (steady conduction equation) over relaxation is preferred. Whatsoever the case may be the value of $\beta$ should be more than 0 and less than 2. One iteration is called to be completed when all the grid points have been visited by Eq. 15. Python 3.7 has been used to solve the above equations numerically and the converged temperature results obtained were shown after adding $T_\infty$ to the $\theta$ (so that we can get the exact temperature not the temperature difference).

**Setting Up Python Code**

- Importing pylab module and setting up font for figures:

```
from pylab import *

    font = {'family' : 'Times New Roman','size': 16}

rc('font', **font)
```

- Supplying input data

```
h=100.0
k=385.0
T=100.0

T_o=30.0

θ=T-T_o
ℓ =6*10**(-2)
R=0.2*10**(-2)
```

- Grid generation

```
nc=10
nr=10
Δz= /(nc-1)
```

Research and Applications of Thermal Engineering
Volume 4 Issue 3
DOI: https://doi.org/10.5281/zenodo.6345803

```
Δr=R/(nr-1)
Ae=AwΔr
An=As=Δz
z=linspace(0, ,nc)
r=linspace(0,R,nr)
r=flipud(r)
```

- Initial Guess for temperature field and boundary conditions

```
θ =zeros((nr,nc))
θ[0,:]= [1,:]/(1+h*Δr/k)#Top
θ[-1,:]= [-2,:]# Bottom
θ[:,0]= _o
θ[:,-1]= [:,-2]/(1+h*Δz/k)#Top
```

- Setting current guess as old value for next iteration error calculations

```
θ_old= θ.copy()
```

- Setting up convergence criterion, iteration count and relaxation factor

```
β=1.8
error=1
count=0
ϵ =1.E-5
```

- Iteration loop

```
while error>ϵ :
                    for iin range(1,nr-1):

for jin range(1,nc-1):

a_E=Ae*r[i]/Δz

a_W=Aw*r[i]/Δz

rn=(r[i]+r[i-1])/2

rs=(r[i]+r[i+1])/2

a_N=An*rn/Δr

a_S=As*rs/Δr
```

Research and Applications of Thermal Engineering
Volume 4 Issue 3
DOI: https://doi.org/10.5281/zenodo.6345803

```
a_P=a_E+a_W+a_N+a_S

Σaθ =a_E*θ[i,j+1]+a_W*θ[i,j-1]+a_N*θ[i-1,j]+a_S*θ[i+1,j]
θ[i,j]=θ_old[i,j]+(β/a_P)*(Σaθ -a_P*θ_old[i,j])

# evaluating error
error=sum(abs(θ -θ_old))

figure(1)

if count%5000==0:

semilogy(count,error,'k-o')

print(error)

# Updating boundary conditions

θ[0,:]=θ[1,:]/(1+h*Δr/k)#Top

θ[-1,:]=θ[-2,:]# Bottom

θ[:,0]=θ_o

θ[:,-1]=θ[:,-2]/(1+h*Δz/k)#Top
# Setting up current value of θ as guess for next iteration
θ_old= θ.copy()

count=count+1
```

- Data Plotting

```
T= θ+T_o
# Contour plot

figure(2,figsize=(10,3),dpi=300)
```

- `contourf(z,r,T,12,cmap='gnuplot')`
- `xlabel('z')`
- `ylabel('r')`
- `colorbar()`
- `savefig('contour.jpg')`

```
# Temperature plot

figure(3,figsize=(10,3),dpi=300)
```

Research and Applications of Thermal Engineering
Volume 4 Issue 3
DOI: https://doi.org/10.5281/zenodo.6345803

•

```
plot(z,T[int(nr/2),:],'r-o')

show()
```

**OBSERVATIONS, RESULTS, AND DISCUSSION**

Figure 3 shows variation of temperature with length of fin for different materials that are Brass, aluminium, copper, respectively.

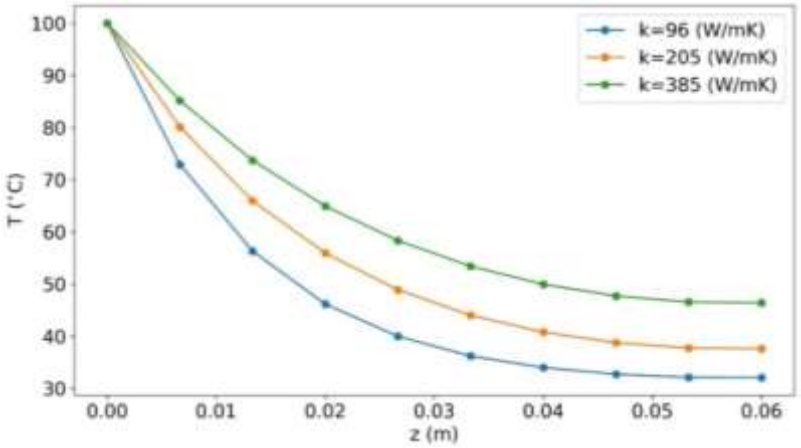


***Fig.3:-****Variation of temperature as a function of fin length.*

Initially, the temperature at the primary wall (i.e., the base of the fin) was 100°C. However, with increasing thermal conductivity, heat transfer increases and higher temperatures are observed throughout the fin surface. Therefore, it is observed that the material with the highest thermal conductivity, i.e. copper has a most elevated temperature at the endpoint of the fin due to high rate of conductive heat transfer along the length of fin. In contrast, the material with the lowest thermal conductivity, i.e., Brass, is observed to resist large amount of heat due to which the fin tip is observed to be very close to atmospheric temperature.

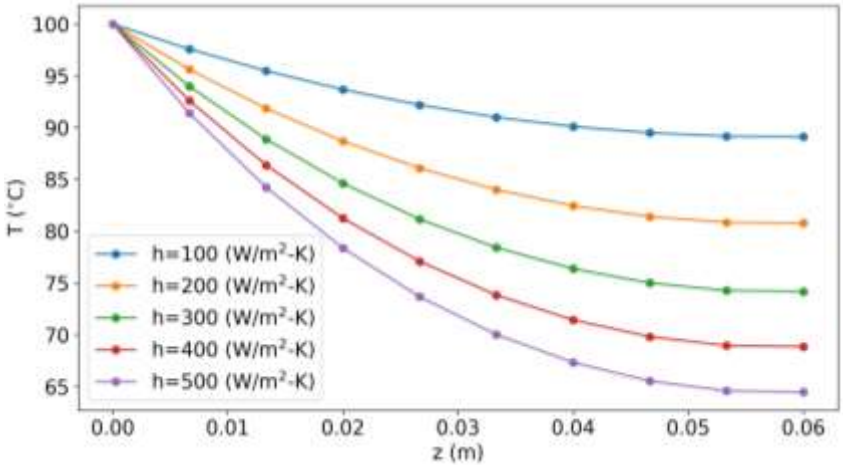


***Fig.4:-****Variation of temperature for Copper with fin length for different enthalpy levels*

Research and Applications of Thermal Engineering
Volume 4 Issue 3
DOI: https://doi.org/10.5281/zenodo.6345803

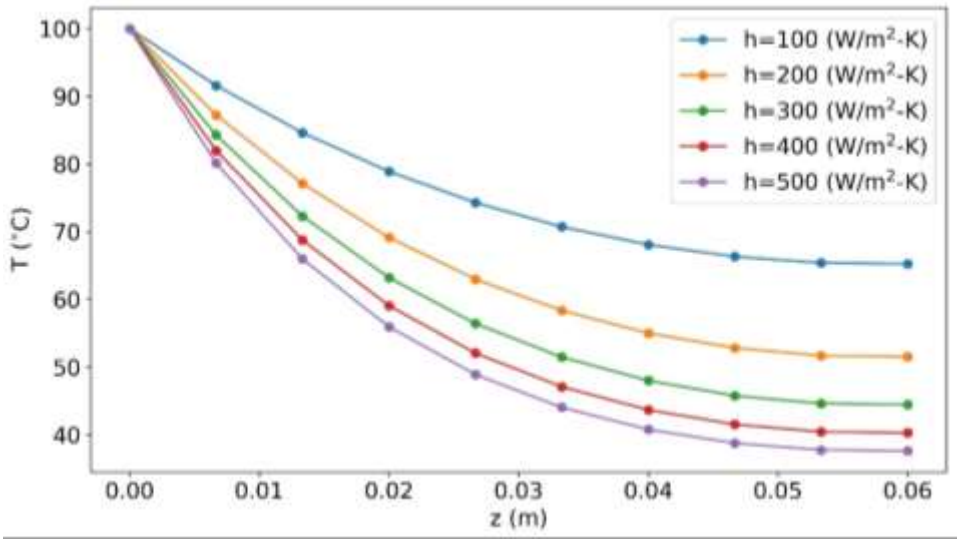


***Fig.5:-****Variation of temperature for Aluminium with fin length for different enthalpy levels*

Figures 4, 5, and 6 show temperature variation with fin length for different surrounding heat transfer coefficients (h) for three other materials, namely Copper, Aluminium, and Brass. Since copper has the highest thermal conductivity, the maximum heat transfer can be observed in it. At *h* of 100 W/m$^2$-K, the heat transfer capacity of a substance is lowest as the temperature at the endpoint of the fin is observed as 89.1°C. While as the h increases, heat distribution throughout the fin via convection increases which can be observed in Figure 4. As the *h* reaches a maximum at 500 W/m$^2$-K, maximum heat distribution can be observed in the material.

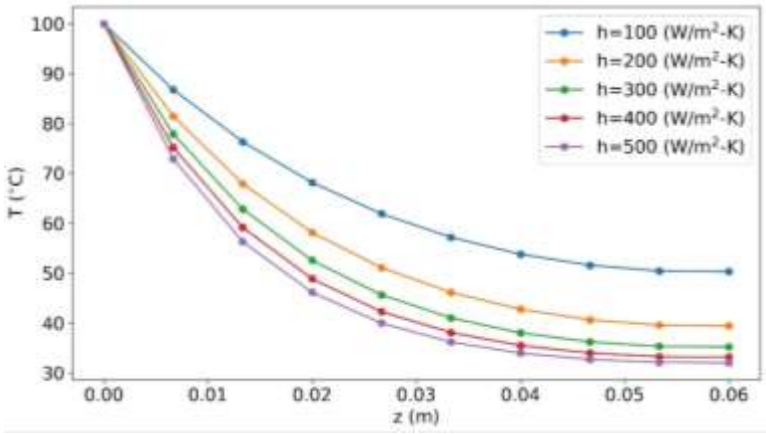


***Fig.6:-****Variation of temperature for Brasswith fin length for different enthalpy levels*

On similar basis, analysis of aluminium and brass was performed which is shown in Figure 5 and 6, respectively. For aluminium, when *h* is lowest temperature at fin tip is observed to be 65.3°C and when *h* reaches highest maximum heat transfer can be observed, where fin tip temperature is observed to be 37.6°C. Similarly for Brass, highest fin tip temperature is found to be 50.3°C with lowest enthalpy, while highest fin tip temperature was observed to be 32.1°C with *h* of 500 W/m$^2$ – K. So, to elevate the heat transfer from the brass fin a substantial high forced convection outside the fin is required.

Research and Applications of Thermal Engineering
Volume 4 Issue 3
DOI: https://doi.org/10.5281/zenodo.6345803

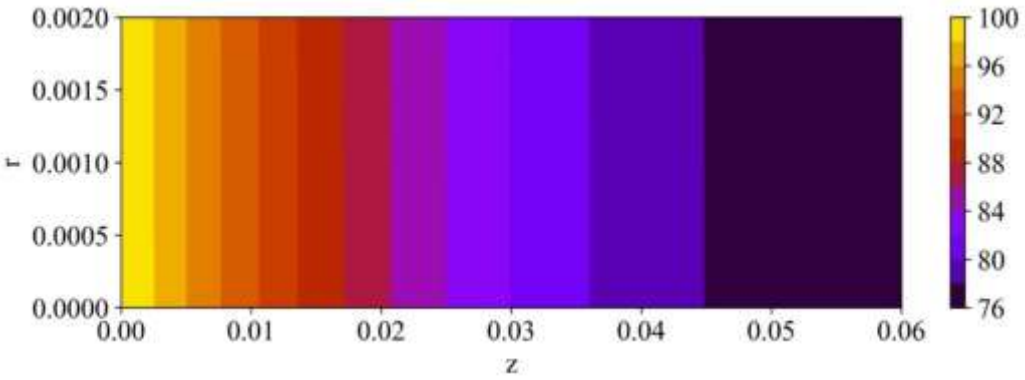


***Fig.7:-****Contour plot*

The Figure 7 show the contour plot of temperature variation within the fin for k = 385 W/m-K and h=100 W/m$^2$-K.It shows that the variation of temperature in the radial direction is not there it is only in length wise direction of the fin. Hence, in all the previous figures temperature was plotted as function of *z*.

Grid independency test has been performed to check the minimum grid size after which the results do not vary much. It has been observed that for a convergence criterion of $10^{-5}$ the results are within a confidence level of 99%for a grid of 10×10.

## CONCLUSIONS

In this analytical study, the numerical heat transfer analysis has been performed on the fin of different material which are exposed to different convective heat transfer coefficients. The variation of temperature has been examined and reported for the different cases.

Where the material used were copper, aluminium, and brass at the convective heat transfer ranges of 100, 200, 300, 400, and 500 W/m$^2$-K, respectively. Based on the numerical computations following conclusions can be drawn:

1. With the increase in thermal conductivity high heat transfer is observed throughout the of fin.
2. For lowest heat transfer coefficient (100 W/m$^2$-K) the value of fin tip temperature for copper, aluminium, and brass fins were 89.1°C, 65.3°C and 50.3°C.
3. For higher heat transfer coefficient, the value of fin tip temperature for copper, aluminium, and brass were 91.2°C, 67.3°C, and 53.1°C, respectively.

## REFERENCES

1. Bahadur, R., & Bar-Cohen, A. (2005, January). Orthotropic thermal conductivity effect on cylindrical pin fin heat transfer. In *International Electronic Packaging Technical Conference and Exhibition* (Vol. 42002, pp. 245-252).
2. M. V. H. S. Kumar,(2018). Experimental Analysis of Natural and Forced Convective Heat Transfer through Cylindrical Pin. 8(440): 440–450.
3. Incropera, F. P., DeWitt, D. P., Bergman, T. L., & Lavine, A. S. (1996). *Fundamentals of heat and mass transfer* (Vol. 6, p. 116). New York: Wiley.
4. Maji, A., & Choubey, G. (2020). Improvement of heat transfer through fins: A brief review of recent developments. *Heat Transfer*, *49*(3), 1658-1685.
5. Maji, A., & Choubey, G. (2020). Improvement of heat transfer through fins: A brief review of recent

developments. *Heat Transfer*, *49*(3), 1658-1685.

6. Lane, H. J., & Heggs, P. J. (2005). Extended surface heat transfer—the dovetail fin. *Applied thermal engineering*, *25*(16), 2555-2565.
7. Agwu Nnanna, A. G., Haji-Sheikh, A., & Agonafer, D. (2003). Effect of variable heat transfer coefficient, fin geometry, and curvature on the thermal performance of extended surfaces. *J. Electron. Packag.* *125*(3), 456-460.
8. Mohankumar, D., Pazhaniappan, Y., Kumar, R. N., Ragul, R., Kumar, P. M., & Babu, P. N. (2021, February). Computational study of heat-transfer in extended surfaces with various geometries. In *IOP Conference Series: Materials Science and Engineering* (Vol. 1059, No. 1, p. 012055). IOP Publishing.
9. Rao, A. K., & Somkuwar, V. (2021). Heat transfer of a tapered fin heat sink under natural convection. *Materials Today: Proceedings*, *46*, 7886-7891.
10. Versteeg, H. K., & Malalasekera, W. (2007). *An introduction to computational fluid dynamics: the finite volume method*. Pearson education.
11. Patankar, S. V. (2018). *Numerical heat transfer and fluid flow*. CRC press.
12. Patankar, S. V. (2018). *Numerical heat transfer and fluid flow*. CRC press.

Cite as

Pankaj Dumka, Saksham Sharma, Harshit Gautam, & Dhananjay R. Mishra. (2022). Finite Volume Modelling of an Axisymmetric Cylindrical Fin using Python. Research and Applications of Thermal Engineering, 4(3), 1–11. https://doi.org/10.5281/zenodo.6345803